Design of Electromechanical Measurement and Control System for Marine Mobile Buoy Based on Neuron PID

Xuan-qun Li[1,2,3](✉) and Ji-ming Zhang[1,2,3]

[1] Institute of Oceanographic Instrumentation, Qilu University of Technology (Shandong Academy of Sciences), Qingdao 266000, China

[2] Shandong Provincial Key Laboratory of Ocean Environmental Monitoring Technology, Qingdao 266000, China

[3] National Engineering and Technological Research Center of Marine Monitoring Equipment, Qingdao 266000, China

Abstract. In order to overcome the shortcomings of buoys that can only observe the marine environment at fixed stations, a neuron PID-based electromechanical measurement and control system design for marine mobile buoys was developed. The overall structure of the hardware equipment of marine mobile buoys was introduced, and a mobile buoy was constructed. Designed a mobile buoy measurement and control system, described the data communication, motion control, and the man-machine interface of the mobile buoy measurement and control system, and gave an example of testing the mobile buoy in the lake. Marine mobile buoys have the ability to autonomously conduct marine environmental observations in a larger area, and are of great value for obtaining large-scale marine environmental information.

Keywords: Neuron PID · Marine mobile buoy · Electromechanical measurement and control

1 Introduction

Among various three-dimensional ocean observation systems, the buoy system is an important marine environment observation equipment. It has the advantages of continuous, long-term and automatic monitoring of marine meteorology and hydrological environment in the harsh marine environment. It is the expansion of marine observation shore base stations, survey ships and survey aircraft in space and time, and has any other surveys. The irreplaceable advantages of the method play a huge role in ocean observation [1]. However, after the buoys are deployed, observations can only be carried out at fixed stations to obtain ocean observation elements near the stations. Relocation and deployment requires a lot of consumption of personnel and ships. The autonomously controlled mobile marine monitoring platform is a powerful tool for in-depth research on the marine environment. Recently, domestic and foreign scholars have proposed the

S. Liu and X. Ma (Eds.): ADHIP 2021, LNICST 416, pp. 689–707, 2022.
https://doi.org/10.1007/978-3-030-94551-0_53

concept of a mobile marine buoy [2]. Designed a marine mobile buoy electromechanical measurement and control system based on neuron PID, using the control of the propeller and rudder and neuron PID technology to realize the monitoring task of the mobile buoy at different stations, and using the digital radio to realize the marine mobile buoy and the shore The control system performs wireless data transmission and communication, and collects various data required [3].

2 Electromechanical Measurement and Control System of Marine Mobile Buoy

2.1 Hardware Structure of Electromechanical Measurement and Control System for Marine Mobile Buoy

The marine mobile buoy can realize the maneuverability of the buoy through the propeller and rudder, and realize the environmental monitoring task of a given sea area through navigation control. It uses solar energy to provide energy and charge the battery, so that the mobile buoy can work stably and reliably for a long time [4]. The marine mobile buoy system consists of the marine part of the mobile buoy and the remote control center. The structure of the marine mobile buoy system is shown in the Fig. 1.

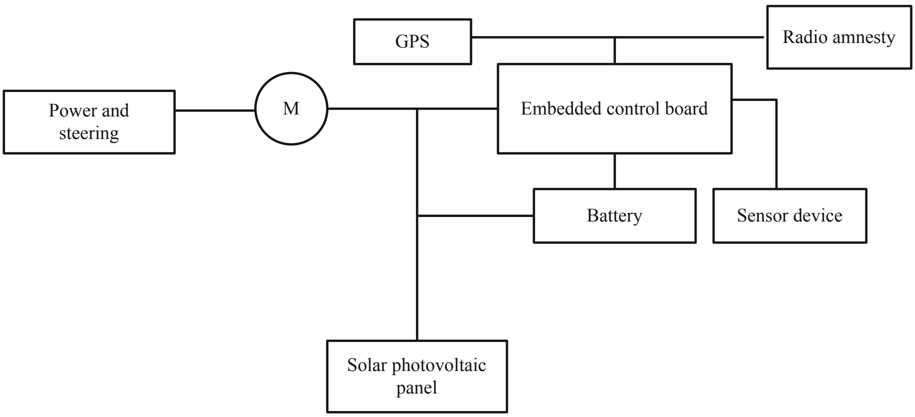

Fig. 1. The structure of the marine mobile buoy maneuvering system

The remote control center is called the upper computer, which can directly issue the control command [5]. The control system of the marine part of the mobile buoy is called the lower computer, which is controlled by the upper computer, and directly controls the function of the mobile buoy. The marine part of mobile buoy is mainly composed of buoy body and embedded control board. By controlling the movement of a hydraulic single degree of freedom experimental platform, the frequency of pressure change of the system is changed. By controlling whether the energy storage is connected to the hydraulic system, the influence of accumulator on different motion frequencies of hydraulic system is studied, and the effect of accumulator on the heave compensation system is verified. The hardware system of the measurement and control system is mainly composed of the upper computer, adlinkpci-8132 motion control card and magnetic grating ruler. The details are shown in the Fig. 2:

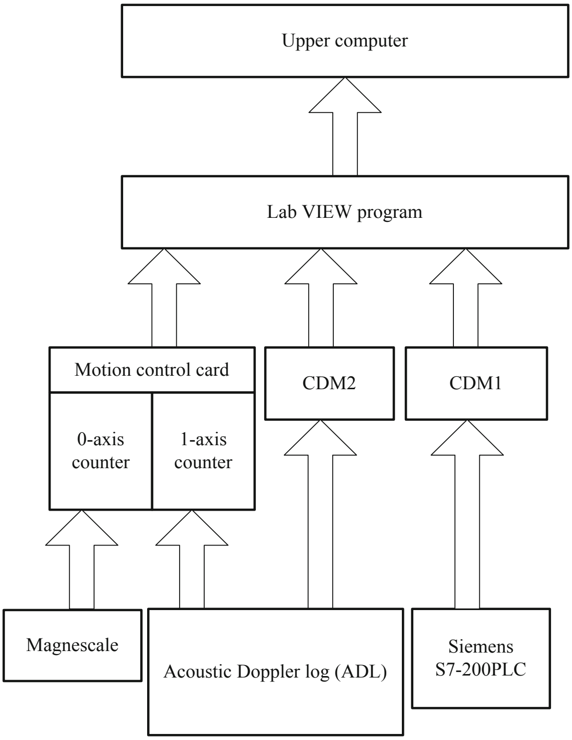

Fig. 2. Overall design block diagram of the system

The single-degree-of-freedom platform is mainly composed of three parts, from left to right: hydraulic station, single-degree-of-freedom actuator, and electronically controlled experimental platform [7]. By operating the electronic control test bench, the movement of the servo cylinder is controlled. The hydraulic station is the power supply unit of the single-degree-of-freedom test bench, which is mainly composed of a motor, a plunger variable pump, an electromagnetic overflow valve, an accumulator, and oil pipes; the single-degree-of-freedom actuator is mainly composed of a servo cylinder and an electro-hydraulic servo valve Composition [8]. The cylinder barrel is fixed, and the movement of the piston rod of the servo cylinder can be controlled by adjusting the voltage of the servo valve [9]. The accumulator is installed at the pump outlet. The composition and principle diagram of the entire hydraulic system are shown in the Fig. 3

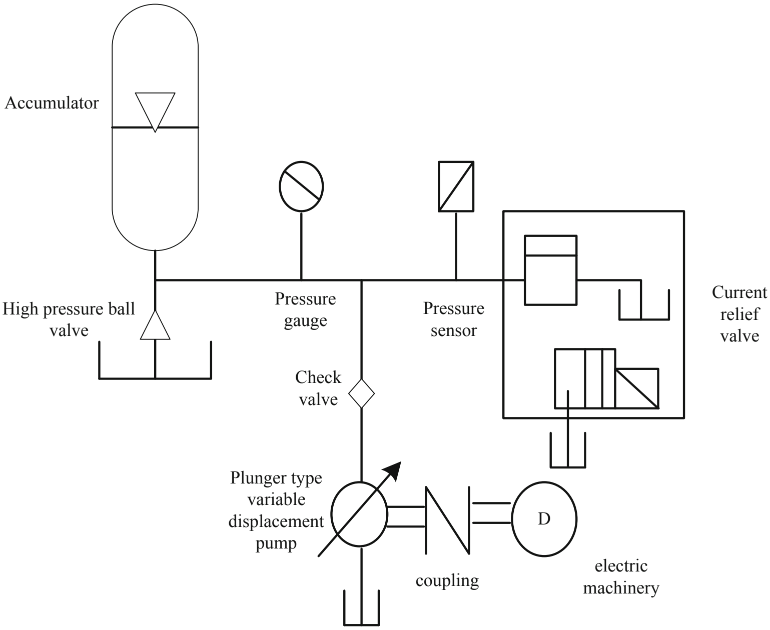

Fig. 3. Hydraulic system power equipment structure

Among them, the power module, motion and direction control module, sensor module, communication module, positioning module and data processing module are integrated on the embedded control main board. Propellers, rudders, solar panels and various sensors are directly installed on the buoy body. The floating part of the marine mobile buoy plays the role of data collection, processing and transmission, and various information collected will be transmitted to the remote control center through wireless communication [10]. The remote control center includes man-machine interface module, data storage module and data communication module. The communication module plays the role of receiving and processing the data sent by the ocean buoy, and transmits the collected data of the ocean buoy to the upper computer in real time to store and display the data. The data displayed include the precise position, heading, speed, sensor data, measurement time, etc. of the marine mobile buoy. In the host computer, by establishing a friendly man-machine interface to process and display the data, the user can conveniently operate the host computer [11]. The electric control experiment platform is mainly composed of a strong current control cabinet, a weak current control cabinet and a computer control system. The strong current control cabinet is used to control the start and stop of the motor and the switch of the electromagnetic overflow valve; the weak current control cabinet and the computer control system are located in the same control cabinet, which are respectively used for the manual and computer control operations of the servo cylinder, and the computer control system realizes the Control of cylinder movement [12]. The computer control system mainly includes computer, PCI-6221 multi-function acquisition card, Moog controller, displacement sensor, pressure sensor, etc. PCI-6221 is used to complete the acquisition and buffering of input signals.

The data is sent to the computer through PCI bus, and the data is processed under the control of application program. At the same time, the command of application software is received, and the electrical signal is sent out to control the action of servo cylinder through MOOG controller. Moog controller as a hardware closed-loop makes the output voltage of PCI-6221 change linearly with the displacement range of the cylinder. The principle of the measurement and control system is shown in the Fig. 4

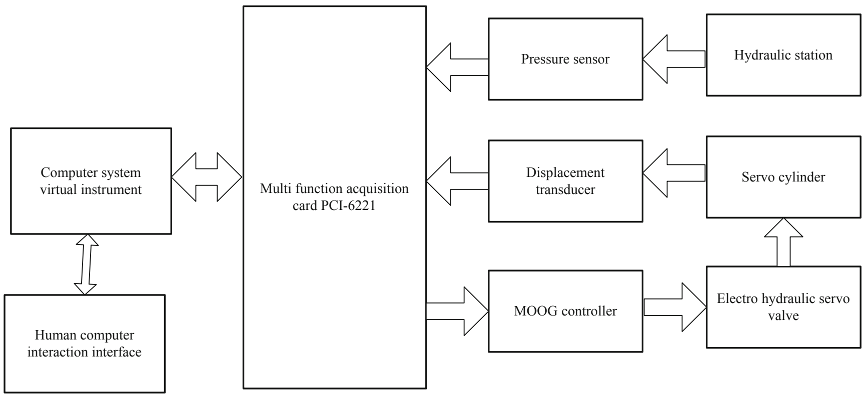

Fig. 4. Perfect function structure of measurement and control system

The specific use process of the measurement and control system is as follows: the displacement signal of the hydraulic cylinder collected by the displacement sensor is input to the controller through the A/D conversion module, and the control voltage signal of the hydraulic cylinder is obtained under a certain control strategy after processing in the controller. The control voltage is converted through the D/a module, and then output to the electronic amplifier, and then output to the electro-hydraulic proportional directional valve, To control the telescopic movement of the hydraulic cylinder. The modular design of the system is essentially the same as the mechanical modular design in the conventional sense, which realizes the overall function of the system through the combination of relatively independent functional modules [13]. However, the combination of mechanical modules is generally guaranteed by mechanical rigid connection, such as bolts, etc., and the combination and Realization of functions are guaranteed by the geometric related conditions between each other. The connection between different modules of the measurement and control system mainly depends on the electrical interface (software) connection to realize the information exchange between modules and complete the relevant control tasks [14]. Therefore, in the modular division and design of the measurement and control system, in order to ensure the reliable operation between modules and improve the reliability of the system, we must follow several criteria: the connection mode and information exchange between modules are simple and reliable. Module functions should be relatively centralized and independent; Module combination should have clear purpose, greater flexibility and good economy [15]. The hardware composition of the six hydraulic cylinders is exactly the same, and the control strategy is responsible for coordinating the telescopic motion of the six hydraulic cylinders to realize the motion of the upper platform. The system is composed of local master station and upper computer, which can realize remote control and data sharing in LAN.

2.2 Function Optimization of System Software

With the continuous development of artificial intelligence control, the artificial intelligence method is used to store the adjustment experience of the operator in the actual operation as knowledge into the computer, and according to the actual situation on the site, the computer can automatically adjust the PID parameters and control, intelligent control Fuzzy control theory in is one of the effective methods to solve this problem [16]. The software system is developed using the LabVIEW graphical programming language of National Instruments. LabVIEW is the most representative graphical programming software in the field of virtual instruments. It is widely used in the fields of testing, process processing and control. The motion control card is used on the LabVIEW development platform. Realizing motion control, data collection is simple and easy (Fig. 5).

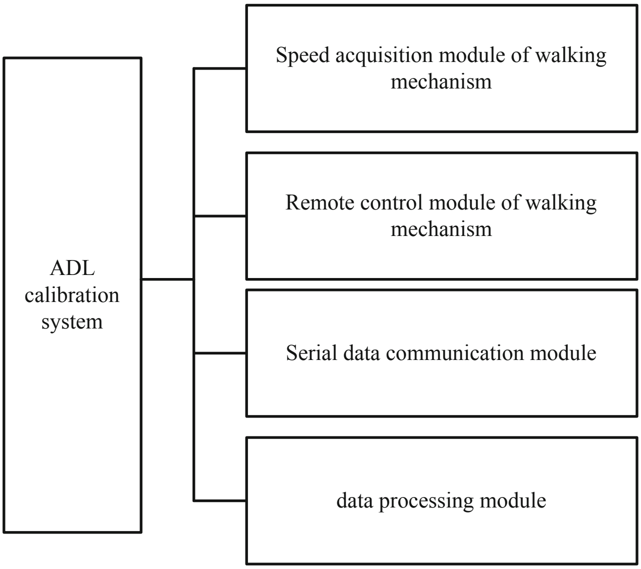

Fig. 5. Software structure block diagram of remote measurement and control system

According to the requirements of the mobile buoy system for the upper computer, it has four main function modules: data communication module, human-computer interface module, data processing module and motion control module. The human-computer interface module is to provide friendly human-computer interface, which is convenient for users to operate. The motion control module mainly controls the motion of Marine Mobile buoy in real time by sending the command to control the marine mobile buoy. The data communication module mainly completes the communication function with the lower computer. The main function of data processing module is to process and store the received data. This paper mainly introduces the human-computer interface module. The man-machine interface module of the upper computer mainly includes the display of the position of the buoy, the track of motion and the parameters in the course of the motion. The position of the motorized buoy is displayed by receiving the GPS information transmitted by the serial port and calling the map. Use the map data as the base map of the map, and use the WebBrowser control in C# to call the JavaScript based program to obtain the map data. The user performs human-computer interaction on the location of geographic information in the electronic map presented by the Web program to obtain the latitude and longitude coordinates of the data object, find the XML information through Xpath, and then update it to the user's special application data [18]. In this software, the latitude and longitude information returned by GPS will be displayed on the map on the left as shown in the figure after being analyzed. GPS keeps sending back data, and will display the track and label on the map in real time. Its specific application will be introduced in the test (Fig. 6).

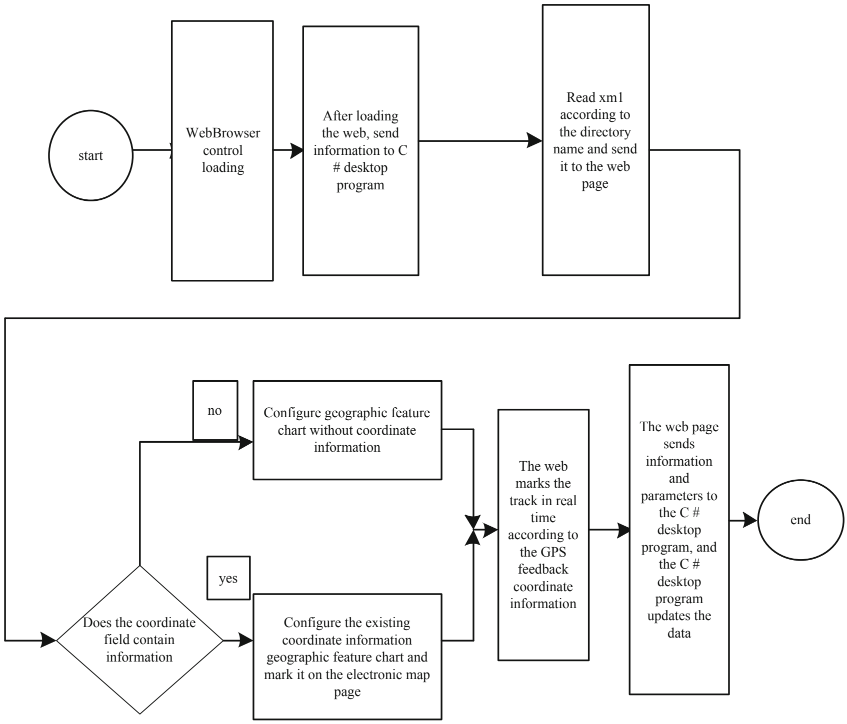

Fig. 6. Optimization of electromechanical measurement and control information call steps

Due to the particularity of marine monitoring and measurement, the mobile buoy must be able to cruise along the given track, reach the designated coordinate position, provide enough energy supply, carry the necessary monitoring equipment, and reach the designated position as fast as possible for various test and monitoring work. The overall size of the motorized buoy is: 2000 mm × 800 mm × 600 mm, and the floating body on the water surface is made of foam floating body material covered with thin steel plate. The power source of the whole device is propeller propulsion, which mainly relies on the rudder to control the direction, and the battery is charged by the solar panel to provide electric power to drive the propeller and rudder board. The motion control module controls the speed of the propeller, the start and stop and the swing angle of the rudder, so that the motion of the maneuverable buoy can be accurately controlled, and the motion of the established trajectory can be realized. In order to clearly display the navigation direction and rudder position of the mobile buoy, a friendly man-machine interface is designed to display the above information. The rudder angle data and the absolute course of the mobile buoy sent back by the lower computer through the data transmission radio will be displayed on the upper computer. At the same time, the upper computer can send commands to the lower computer to control the movement of the mobile buoy. The basic principle of conventional PID control system is shown in the Fig. 7.

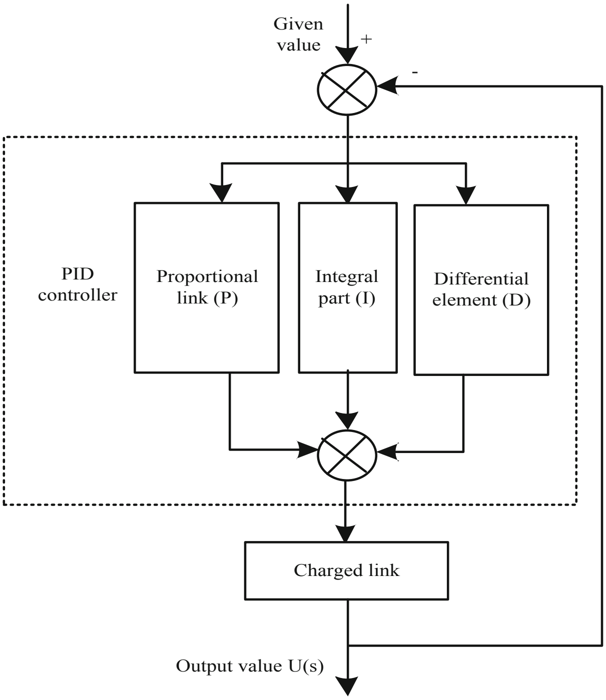

Fig. 7. Basic principle of PID control system

The function of each correction link of PID controller is briefly described as follows: the proportional link reflects the deviation signal of the control system in proportion immediately. Once the deviation is generated, the controller immediately produces a control effect to reduce the deviation. The integral part improves the error free degree of the control system by eliminating the static error; The differential part reflects the variation trend of the deviation signal, and introduces an effective correction signal before the deviation signal becomes too large, so as to speed up the reaction speed of the system and reduce the adjustment time. The selection of PID control parameters should be based on the specific characteristics of the controlled object and the performance requirements of the control system. The basic concept of fuzzy control is mainly used for macro control of the system. It is a computer intelligent control based on fuzzy set theory, fuzzy linguistic variables and fuzzy reasoning. Its basic principle is shown in the figure, and the core part is the fuzzy controller in the dotted diagram (Fig. 8).

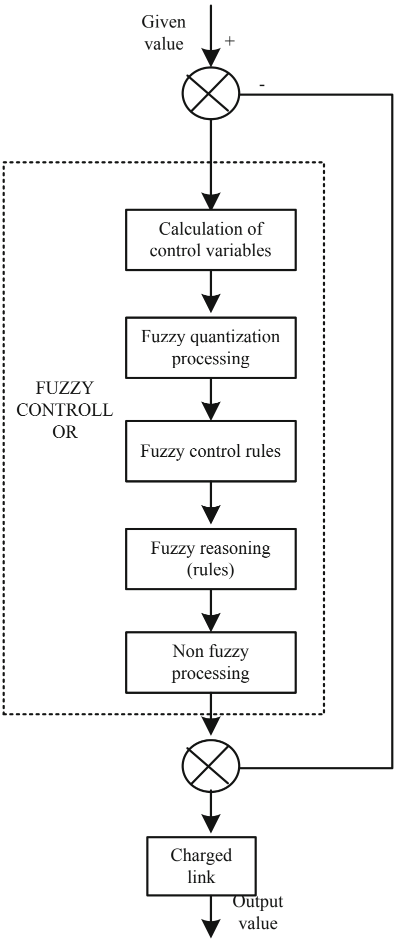

Fig. 8. Measurement and control principle of fuzzy control system

The control law of the fuzzy controller is realized by the computer. The realization process of the fuzzy control algorithm is as follows: First, the computer obtains the precise value of the controlled quantity through sampling, and then compares the precise value with the given value to obtain the deviation signal e, and takes the deviation signal e as the FC An input quantity is fuzzified to become a fuzzy quantity, which is expressed in the corresponding fuzzy language to obtain a subset E of the fuzzy language set of the deviation signal e, which is then obtained by reasoning from E and the fuzzy control rule R (fuzzy relationship) The synthetic rule makes fuzzy decision-making and obtains the fuzzy control U = ER. Finally, the fuzzy quantity U is unfuzzified and transferred to the controlled object for further control. In summary, the fuzzy control algorithm can be briefly summarized as the following four steps:

According to the output value of the system obtained this time, the input variable selected by the system is calculated.

Fuzzy the precise value of the input variable into a fuzzy value.

According to the fuzzy value of the input variable and the fuzzy control law, the fuzzy inference (rule) is performed to calculate the fuzzy value of the control variable.

Unfuzzy the fuzzy control variables obtained, calculate the precise control quantity, control the system, and loop through it.

The overall function diagram of the platform measurement and control system software is as shown (Fig. 9):

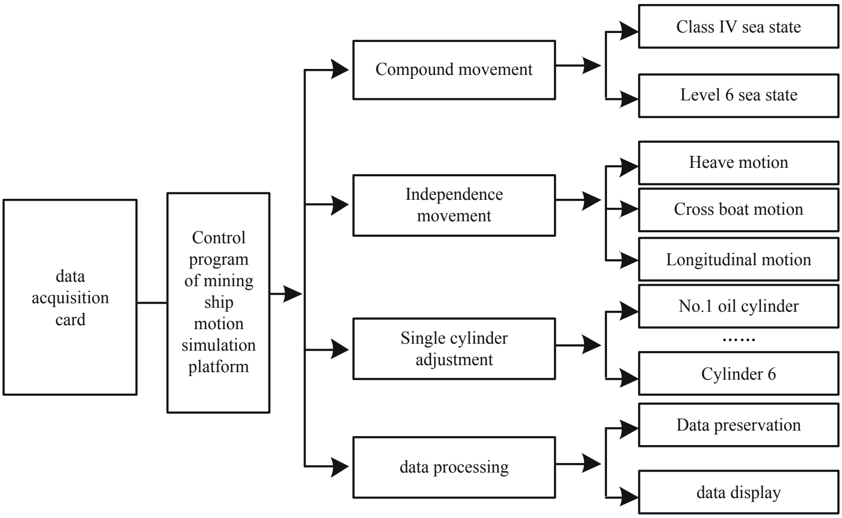

Fig. 9. The overall function of the platform measurement and control system software

In order to complete the various functional requirements of the mobile buoy, the lower-level computer mainly includes the following modules: the position of the mobile buoy is determined by GPS, and the buoy is controlled by the position of the mobile buoy, and the information is collected by the high-precision GPS module. The GPS latitude and longitude information is returned to the embedded control board, and then the information is returned to the upper computer control terminal through the digital radio, which is displayed on the map and the geographic location information is stored. The motorized buoy will be powered by solar panels, and the voltage must be sufficient and usable. The power management module will detect whether the voltage meets the

14 V working voltage and perform various actions when it meets the requirements. At the same time, different voltage values need to be configured to meet the working voltage of each module. The steering gear part and the data transmission station supply 12 V voltage, and the GPS and system voltage supply 5 V voltage, and then the system voltage is distributed to 3 V, 3.3 V, etc. Including propeller motor, steering gear and encoder. The propeller motor can control the start and stop of the marine mobile buoy, and the steering gear and encoder are used to precisely control the steering gear's angle, and then control the steering of the mobile buoy so that it can reach the specified position. The communication module must realize the long-distance.

2.3 Realization of Electromechanical Measurement and Control Management of Marine Mobile Buoy

The waves in my country's deep-sea mining areas are mainly divided into swells and waves. Waves are waves that directly act on the surface of the ocean by wind, and surges are waves that propagate to static waters when the wind and waves leave the wind area. The average annual wind speed in my country's mining areas is equivalent to Grade 4. Tropical storms and typhoons mainly occur in summer. According to foreign meteorological statistics, the average annual wind speed in the three months of July, August and September is 3.6–4.4 and 2.9, and the annual average is 15 times, each lasting 1–2 days. Therefore, tropical storms and typhoons will affect mining operations for 30–40 days a year. According to a 1994 survey by the Ministry of Geology "Ocean No. 4", the average wind wave height during exploration in China's mining areas was 0.7 m. Small waves account for 52%, light waves 40%, medium waves 8%, and big waves only 0.3%. The frequency of mid surge is 86%, the maximum surge wave height is 2.5 m, and the probability of occurrence is very small. The higher the wave height of a sea wave, the longer its period and wavelength, and vice versa. For example, the period of medium waves is 3.647 s; strong waves are 5.8–7.2 s. The sea surface water velocity in the mining area is about 0.33 m/s, the water temperature is about 250 C, the seabed water velocity is 0.18 m/s, and the water temperature is 1–20 C. Since the sea wave condition is the most concerned issue during the mining operation, the statistics of the surge condition in the C-C area are made as shown in the (Tables 1 and 2).

Table 1. Sea state characteristics survey statistics table

Sea state	Wave height (m)	Frequency of occurrence (%)
Maximum surge	2.5	Minimum
Chung Chung	0.819	86
Big wave	>2	0.3
Mid wave	1.319	8
Light waves	0.812	40
Xiaolang	0.307	52

Table 2. Wave characteristics of sea conditions of class 4 and 6 H**1/3**

Sea state	Mean wave height (m)	Average wind speed (m/s)	Meaningful wave height $H_{1/3}$ (m)	Period (s)
Level 6	4.9	18	6	8.8–10
Level 4	2	9	2.4	4.7–5.8

From the analysis of the table, we can see that the overall surge conditions in my country's mining areas are good, with small light waves and moderate waves as the main ones, and severe sea conditions are rare. Therefore, the prerequisite for the design of my country's deep-sea mining system is that the system can perform normal operations under four-level sea conditions and stop operations under six-level sea conditions. That is, the mining ship simulation system needs to simulate the movement characteristics of the mining ship under four-level and six-level sea conditions. The wave height in the table refers to the vertical height between the peak of a separate wave and the adjacent trough; the average wave height refers to the average value of all wave heights and the average value of all wave heights observed through the stationary observation point during the observation point observation period; Significant wave height refers to the average value of the maximum wave height observed through a stationary observation point. Assuming that the propagation direction of ocean waves is constant, and the crest and trough lines are parallel to each other and perpendicular to the propagation direction, such ocean waves are called binary irregular waves, or long-peak waves, and are denoted as ε_i. The modeling and simulation of binary irregular long peak waves have been widely used in ship motion control systems. The Longuet-Higgins model is used to analyze the two-dimensional irregular long-peak wave ocean wave spectrum. It is believed that it can be described by the superposition of countless cosine waves with different periods and initial phases. The expression of the wave equation at a certain fixed position is:

$$\xi(t) = \sum_{i=1}^{N} \alpha_i \cos(\omega_i t + \varepsilon_i) \tag{1}$$

The relationship between the amplitude a of each harmonic wave and the wave spectrum ω_i is as follows:

$$a_i = \sqrt{2S(\omega_i)\Delta\omega_i - \xi(t)} \tag{2}$$

Therefore, the wavefront equation of the long peak wave can be obtained as:

$$\xi(t) = \sum_{i=1}^{N} \sqrt{2S(\omega_i)\Delta\omega} \cos(\omega_i t + a_i \varepsilon_i) \tag{3}$$

It can be obtained from the derivation of the three basic parameters x of the proportional valve flow-pressure equation P, the hydraulic cylinder flow continuity index V and the hydraulic cylinder dynamic equation. The forward and reverse motion parameters β

of the asymmetric cylinder need to be selected according to the direction of motion A. Corresponding equations, in mathematical modeling, cannot reflect the characteristics of the sudden change in pressure C and asymmetry w of the two chambers of the hydraulic cylinder when the valve-controlled cylinder system commutation movement, which is not conducive to simulation calculations.

$$\begin{aligned}&\frac{C_d w_1 x_v}{2}\left[(1+\text{sign}(x_v))\cdot\text{sign}(P_s-P_1)\sqrt{\frac{2}{\rho}|P_5-P_1|}-(1-\text{sign}(x_v))\cdot\text{sign}(P_1-P_0)\sqrt{\frac{2}{\rho}|P_1-P_0|}\right]\\&-C_i(P_1-P_2)-C_eP_1=A_1\dot{x}_5+\frac{V_1}{\beta_e}\dot{P}_1\end{aligned} \tag{4}$$

Further establish the nonlinear equation of the system as:

$$\begin{cases}\dot{X}_1=X_2\\ \dot{X}_2=\frac{A_1}{M}X_3-\frac{A_2}{M}X_4-\frac{B}{M}X_2-\frac{K}{M}X_1+\frac{1}{M}F_L\\ \dot{X}_3=g_1U-\frac{\beta_{\in}A_1}{V_1}X_2-\frac{\beta_eC_i}{V_1}(X_3-X_4)-\frac{\beta_eC_e}{V_1}X_3\\ \dot{X}_4=g_2U+\frac{\beta_eA_2}{V_2}X_2-\frac{\beta_eC_i}{V_2}(X_3-X_4)-\frac{\beta_eC_e}{V_2}X_4\\ x_s=X_1\end{cases} \tag{5}$$

In order to maintain the integrity of the physical meaning of the entire system, in the co-simulation system constructed in this paper, the second working mode of the hydraulic cylinder is adopted, that is, the speed and displacement of the piston rod relative to the hydraulic cylinder are calculated by the ADAMS dynamic model. Output to the EASYS model; in this way, the EASYS hydraulic system calculates the pressure in the upper and lower oil chambers of the hydraulic cylinder and the pressure in the accumulator according to the given speed and displacement at each step of the simulation iteration; at the same time, EASYS will calculate the pressure in the upper and lower oil chambers of the hydraulic cylinder according to the given speed and displacement. The difference and the damping force caused by the speed, calculate the hydraulic driving force acting on the piston by the hydraulic system. The ADAMS model uses the hydraulic driving force as an input signal for dynamic calculations. This completes the data exchange of the co-simulation process. The simulation results of the hydraulic model of the co-simulation can be viewed in EASYS, and the dynamic model, which is the simulation result of the platform movement, can be viewed in ADAMS. The co-simulation schematic diagram and the co-simulation process are shown in the Fig. 10.

The three software used by the system, namely EASYS, ADAMS and MatLAB, need to be installed in the root directory of the hard disk, such as C:}IVIATLAB701, and the installation directory must not contain spaces and Chinese, otherwise EASYS cannot find the necessary during the compilation process The file is compiled. When installing EASYS and ADAMS, choose CompaqVisualFortran6 as the software compiler. During the software installation process, the software compiler settings for EASYS and ADAMS have been carried out. After the installation is complete, you need to set up the MatLAB compiler. Type mex-setup in the MatLAB command window, and select Microsoft Visual C++ 6.0 as the compiler for co-simulation. In this way, the effective use of the control system is realized, and the operation effect and function of the system are improved.

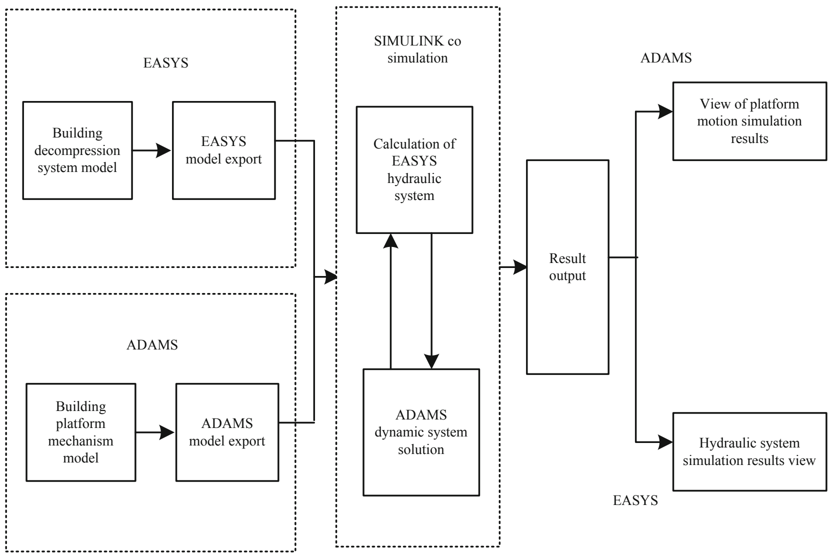

Fig. 10. Optimization of system operation steps

3 Analysis of Results

Use the STK simulation buoy to communicate with the ARGOS satellite to generate the data needed for the experiment (Figs. 11 and 12).

Through STK scene simulation, under different radiation source coordinates, simulation data such as the speed and position of the satellite and the received Doppler frequency can be obtained at different times.

An electromechanical measurement and control system for marine mobile buoys based on neuron PID is proposed. In order to verify the function of the system, a comparative test was performed compared with the traditional system. From the conclusion of the simulation analysis, it can be seen that the passive system with accumulator has a better compensation effect on high frequency waves, but the compensation effect for low frequency is poor, and the compensation rate is even negative. That is, the accumulator has a negative effect on high frequency waves. Hydraulic shock has a better absorption effect, and for low-frequency pulsation, because the process of storing and releasing energy is faster than the process of system pressure change, it will be difficult to play a good role, and sometimes even a negative effect. Refer to the explanations of some inherent parameters of the hydraulic system in the product description of the hydraulic drive system of the deep-sea mining ship motion simulation platform, and set the parameters of the mathematical model of the valve-controlled non-stack symmetrical system. The above-mentioned valve-controlled cylinder system is used as the construction For the model object, the parameter estimation table of the nonlinear mathematical model is as follows (Table 3):

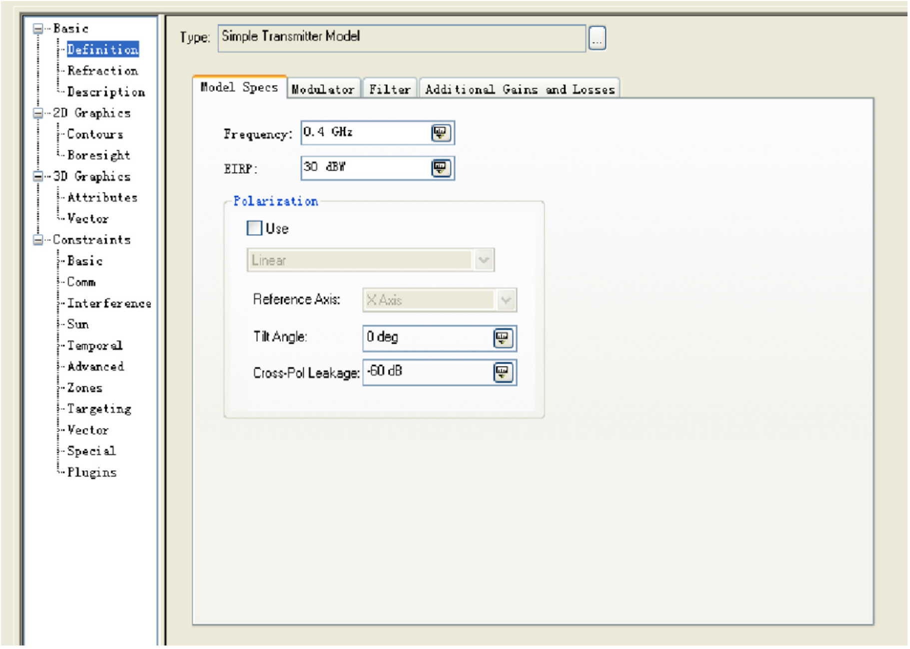

Fig. 11. STK radiation source setting diagram

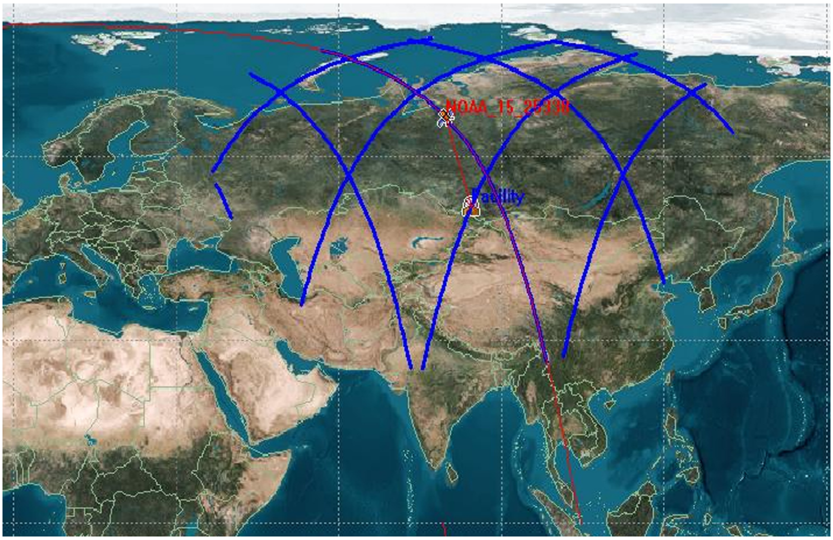

Fig. 12. Schematic diagram of STK two-dimensional simulation

Table 3. Non-linear mathematical model parameter estimation table

Parameter name	Parameter value (unit)	Parameter name	Parameter value (unit)
C_d	0.67	V10	3.216e−4 (m^3)
A_1	5.026e−3 (m^2)	V20	2.110e−1 (m^3)
A_2	2.513e−3 (m^2)	P_S	11 MPa
B	850 (N·s/m)	C_e	7.654e−13 (m/s·Pa)
β_e	750 (MPa)	C_1	2.863e−13 (m/s·Pa)
W_2	1.88e−2 (m)	M	100 (Kg)
W_1	3.76e−2 (m)	P	0.875e3 (kg/m^3)

Through Matlab/Simulink toolbox, the nonlinear mathematical model of the valve-controlled cylinder system is established, and the S-function is introduced to describe the nonlinear model. Substitute the estimated values of model parameters in the table to simulate the nonlinear model. The communication function of the marine mobile buoy mainly sends control commands through the upper computer control center to control the movement of the mobile buoy. This test reflects the communication function through the test of wireless communication performance. Mainly to test the wireless module program of the mobile buoy, the wireless drive module can send and receive data correctly and timely. The lower computer and the upper computer of the marine mobile buoy communicate by means of digital radio, and the maximum transmission distance is 20 km. During the test, the motorized buoy was placed in an open lake, and at the same time, a computer installed with the upper computer monitoring center software sent control commands to the marine mobile buoy. First turn on the power supply, turn on the main control board, initialize the wireless module, then turn on the host computer monitoring center, after the setting is completed, the wireless connection is performed, and finally the start control command is sent. At this time, the marine mobile buoy can move in the lake. At the same time, the host computer monitoring center can receive the neuron PID and other information sent back by the marine mobile buoy in real time. The marine mobile buoy can move according to the control instructions issued by the upper computer monitoring center, and the upper computer monitoring center can also receive the data fed back by the marine mobile buoy. In order to ensure that the identified model has higher reliability, the system input signal must meet the following conditions: during the test period, the input signal can continuously stimulate the system to produce a response, and can excite the modes within the working range of the system. The working condition of the simulation platform is required to reflect the motion curve within the frequency 0.5. In order to be able to build a model closer to the actual working condition, select the same control quantity input to obtain the comparison between the displacement output of the nonlinear model and the displacement output measured by the experiment as the picture shows (Figs. 13 and 14):

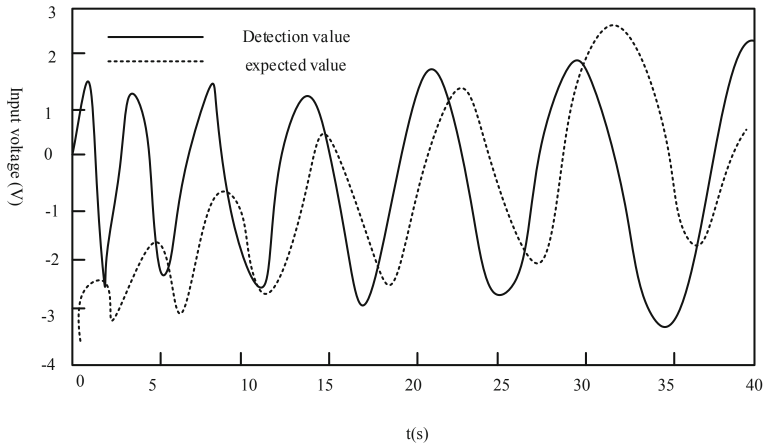

Fig. 13. Traditional method detection results

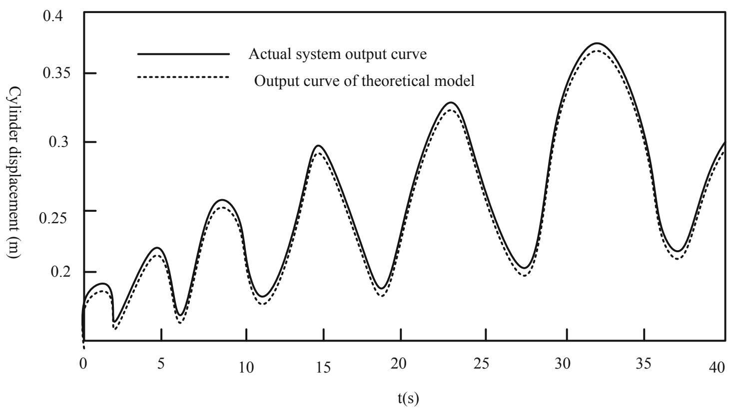

Fig. 14. Test results of the method in this paper

The upper computer control center sends the set target position to the marine mobile buoy in the form of coordinates. Then the marine mobile buoy will perform corresponding movement according to the program setting after receiving the start control command. The test result is shown in the Fig. 15.

In the actual test, the movement of the marine mobile buoy can be controlled through the upper computer monitoring center. After setting the target position of the movement in the monitoring center of the upper computer, the main control board of the lower computer controls the motor and the propeller drives the movement of the marine mobile buoy. At the same time, it controls the steering gear to adjust the direction of the marine mobile buoy.

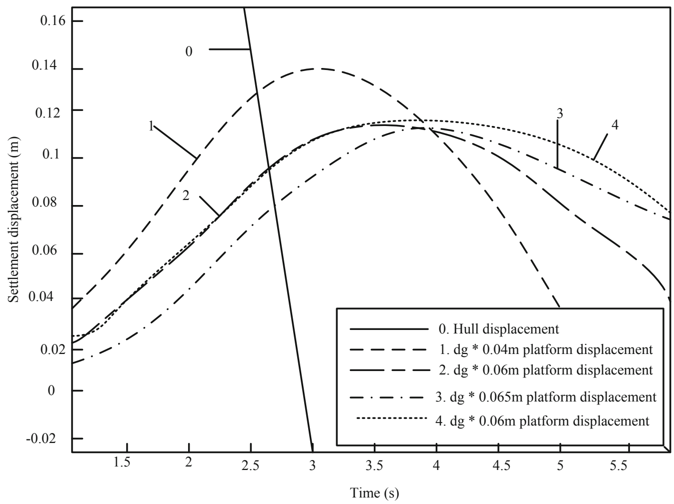

Fig. 15. The influence of different pipe diameters on the heave compensation effect

It can be seen from the figure that the theoretical model output response curve of the nonlinear mathematical model established in this paper is basically consistent with the actual system output response curve trend, reflecting the effectiveness of the nonlinear mathematical model of the above-mentioned motion simulation platform, and it can be used as a valve-controlled cylinder A theoretical research platform for performance analysis in all aspects, to conduct research and analysis on control strategies and other aspects. The results of the experiment show that the motorized buoy can realize its motion control, positioning, data transmission and other functions through remote control. The movement of the motorized buoy in the lake can be accurately represented on the map, with high resolution and strong reliability.

4 Concluding Remarks

This paper develops a neuron PID-based electromechanical measurement and control system for marine mobile buoys that can monitor a wide range of marine environment, completes the mechanical structure design and measurement and control system design of marine mobile buoys, and compiles the embedded control board and the various modules. Program design. The system realizes the functions of remote control, positioning, information transmission and display of the mobile buoy, and can be equipped with various monitoring instruments for marine environment monitoring, and has strong practicability.

On the basis of this system, more comprehensive monitoring content can be added to facilitate testing of newly designed buoys, reducing experiment costs and experiment time.

References

1. Knight, P.J., Cai, O.B., Sinclair, A., et al.: A low-cost GNSS buoy platform for measuring coastal sea levels. Ocean Eng. **203**(9), 107198 (2020)
2. Palm, J., Eskilsson, C.: Mooring systems with submerged buoys: influence of buoy geometry and modelling fidelity. Appl. Ocean Res. **102**(10), 102302 (2020)
3. Ghiasi, M., Soares, C.G.: Influence of the shape of a buoy on the efficiency of its dual-motion wave energy conversion. Energy **214**(118998) (2020)
4. Ma, Y., Mao, Z.Y., Qin, J., et al.: A quick deployment method for sonar buoy detection under the overview situation of underwater cluster targets. IEEE Access **PP**(99), 1 (2019)
5. Wei, X., Liu, N., Dong, T., et al.: A preliminary assessment of an innovative air-launched wave measurement buoy. Appl. Ocean Res. **106**(1–2), 102458 (2020)
6. Numerical Study on the Optimization Design of the Conical Bottom Heaving Buoy Convertor. Ocean Engineering **173**(FEB.1), 235–243 (2019)
7. Xi, F., Pang, Y., Liu, G., et al.: Self-powered intelligent buoy system by water wave energy for sustainable and autonomous wireless sensing and data transmission. Nano Energy **61**(8), 1–9 (2019)
8. Lerch, M., De-Prada-Gil, M., Molins, C.: The influence of different wind and wave conditions on the energy yield and downtime of a Spar-buoy floating wind turbine. Renewable Energy **136**, 1–14 (2019)
9. Li, M., Wu, B.J., Jiang, C.Y., et al.: Effect of reciprocating and unidirectional airflow on primary conversion of a pentagonal Backward Bent Duct Buoy. Appl. Ocean Res. **89**, 85–95 (2019)
10. Tna, B., Rk, B., Rn, A., et al.: Numerical analysis of boundary conditions in a Lagrangian particle model for vertical mixing, transport and surfacing of buoyant particles in the water column. Ocean Model. **136**, 107–119 (2019)
11. Jullien-Corrigan, A., Ahmadi, K.: Measurement of high-frequency milling forces using piezoelectric dynamometers with dynamic compensation. Precis. Eng. **66**(9), 1–9 (2020)
12. Silva-Saravia, H.D., Pulgar, H.A., Tolbert, L.M., et al.: Enabling utility-scale solar PV plants for electromechanical oscillation damping. IEEE Trans. Sustainable Energy **PP**(99), 1 (2020)
13. Wang, R., Gao, J., Li, S., et al.: Condition-based dynamic supportability mechanism for the performance quality of large-scale electromechanical systems. IEEE Access **PP**(99), 1 (2020)
14. Yang, D., Zhang, T., Cai, G., et al.: Synchrophasor-based dominant electromechanical oscillation modes extraction using OpDMD considering measurement noise. IEEE Syst. J. **13**(3), 3185–3193 (2019)
15. Luo, Q., Guo, Z., Huang, H., et al.: Nanoelectromechanical switches by controlled switchable cracking. IEEE Electron Device Lett. **40**(99), 1209–1212 (2019)
16. Bordone, A., Ciuffardi, T., Raiteri, G., et al.: Improved current estimates from spar buoy-mounted ADCP measurement station: a case study in the Ligurian sea. J. Marine Sci. Eng. **9**(5), 466 (2021)
17. Hu, Z., Wu, T.: Research on multidimensional information collection algorithm of marine buoy wireless communication network. Microprocessors Microsyst. **80**(2), 103582 (2021)
18. Gish, L.A.: Concept design of a deployable marine energy testing system. Marine Technol. Soc. J. **54**(6), 84–90 (2020)